

1 **Prime hAd5 Spike + Nucleocapsid Vaccination Induces Ten-Fold Increases in Mean T-Cell**  
2 **Responses in Phase 1 Subjects that are Sustained Against Spike Variants**

3  
4 Peter Sieling<sup>1</sup>, Thomas King<sup>1</sup>, Raymond Wong<sup>1</sup>, Andy Nguyen<sup>1</sup>, Kamil Wnuk<sup>1</sup>, Elizabeth  
5 Gabitzsch<sup>1</sup>, Adrian Rice<sup>1</sup>, Helty Adisetiyo<sup>1</sup>, Melanie Hermreck<sup>1</sup>, Mohit Verma<sup>1</sup>, Lise Zakin<sup>1</sup>,  
6 Annie Shin<sup>1</sup>, Brett Morimoto<sup>1</sup>, Wendy Higashide<sup>1</sup>, Kyle Dinkins<sup>1</sup>, Joseph Balint<sup>1</sup>, Victor Peykov<sup>1</sup>,  
7 Justin Taft<sup>2,5,6</sup>, Roosheel Patel<sup>2,3</sup>, Sofija Buta<sup>2,3,4</sup>, Marta Martin-Fernandez<sup>2,3,4,5,6</sup>, Dusan  
8 Bogunovic<sup>2,3,4,5,6</sup>, Patricia Spilman<sup>1</sup>, Lennie Sender<sup>7</sup>, Sandeep Reddy<sup>7</sup>, Philip Robinson<sup>8</sup>, Shahrooz  
9 Rabizadeh<sup>1</sup>, Kayvan Niazi<sup>1</sup>, and Patrick Soon-Shiong<sup>1\*</sup>

10

11 **Affiliations**

12 <sup>1</sup>ImmunityBio, LLC, 9920 Jefferson Blvd., Culver City, CA 90232, USA

13 <sup>2</sup>Center for Inborn Errors of Immunity, <sup>3</sup>Department of Pediatrics, <sup>4</sup>Precision Immunology

14 Institute, <sup>5</sup>Mindich Child Health and Development Institute, <sup>6</sup>Department of Microbiology, Icahn

15 School of Medicine at Mount Sinai, 1 Gustave Lane, Levy Place, New York, NY 10029-5674,

16 USA SPA

17 <sup>7</sup>NantKwest, Inc., 9920 Jefferson Blvd., Culver City, CA 90232, USA

18 <sup>8</sup>Hoag Hospital, Newport Beach, CA 92663, USA

19

20 \*Corresponding author: [Patrick@Nantworks.com](mailto:Patrick@Nantworks.com)

21

22 **Keywords:** hAd5 Spike + Nucleocapsid, T cells, variants, SARS-CoV-2, COVID-19, vaccine

23

24

25

26 **ABSTRACT**

27 In response to the need for a safe, efficacious vaccine that elicits vigorous T cell as well as  
28 humoral protection against SARS-CoV-2 infection, we have developed a dual-antigen COVID-19  
29 vaccine comprising both the viral spike (S) protein modified to increase cell-surface expression  
30 (S-Fusion) and nucleocapsid (N) protein with an Enhanced T-cell Stimulation Domain (N-ETSD)  
31 to enhance MHC class I and II presentation and T-cell responses. The antigens are delivered using  
32 a human adenovirus serotype 5 (hAd5) platform with E1, E2b, and E3 regions deleted that has  
33 been shown previously in cancer vaccine studies to be safe and effective in the presence of pre-  
34 existing hAd5 immunity. The findings reported here are focused on human T-cell responses due  
35 to the likelihood that such responses will sustain efficacy against emerging variants, a hypothesis  
36 supported by our *in silico* prediction of T-cell epitope HLA binding for both the first-wave SARS-  
37 CoV-2 ‘A’ strain and the B.1.351 strain K417N, E484K, and N501Y spike and T201I N variants.  
38 We demonstrate the hAd5 S-Fusion + N-ETSD vaccine antigens expressed by previously SARS-  
39 CoV-2-infected patient dendritic cells elicit Th1 dominant activation of autologous patient T cells,  
40 indicating the vaccine antigens have the potential to elicit immune responses in previously infected  
41 patients. For participants in our open-label Phase 1b study of the vaccine (NCT04591717;  
42 <https://clinicaltrials.gov/ct2/show/NCT04591717>), the magnitude of Th-1 dominant S- and N-  
43 specific T-cell responses after a single prime subcutaneous injection were comparable to T-cell  
44 responses from previously infected patients. Furthermore, vaccinated participant T-cell responses  
45 to S were similar for A strain S and a series of spike variant peptides, including S variants in the  
46 B.1.1.7 and B.1.351 strains. The findings that this dual-antigen vaccine elicits SARS-CoV-2-  
47 relevant T-cell responses and that such cell-mediated protection is likely to be sustained against  
48 emerging variants supports the testing of this vaccine as a universal booster that would enhance  
49 and broaden existing immune protection conferred by currently approved S-based vaccines.

50

## 51 INTRODUCTION

52 To address the need for an efficacious COVID-19 vaccine that elicits broad immunity against  
53 SARS-CoV-2 and has a high likelihood of maintaining efficacy against emerging SARS-CoV-2  
54 variants, we have developed a dual-antigen COVID-19 ‘T-cell’ vaccine. This dual-antigen vaccine  
55 expresses both the virus spike (S) and nucleocapsid (N) proteins using a next-generation human  
56 adenovirus serotype 5 (Ad5) platform. The S antigen is full-length S including SD1 receptor  
57 binding domain, S1 and S2 domains modified to enhance surface expression (S-Fusion);<sup>1</sup> and full-  
58 length N protein modified with an Enhanced T-cell Stimulation Domain (ETSD) to direct N to the  
59 endo/lysosomal compartment for increased MHC class I and II expression. The hAd5 platform has  
60 deletions in the E1, E2b, and E3 gene regions, thereby minimizing host anti-vector immune  
61 responses<sup>2,3</sup> and enabling efficient antigen cargo expression and cognate T-cell activation even in  
62 the presence of existing anti-adenovirus immunity, as demonstrated previously in clinical studies  
63 targeting tumor-associated antigens in cancer patients.<sup>4,5</sup>

64 The emergence of SARS-CoV-2 variants that have the potential to evade immune responses  
65 generated in response to currently available vaccines has spurred renewed interest in the potential  
66 role of T cells in conferring long-term protection against COVID-19.<sup>6-9</sup> SARS-CoV-2 vaccine  
67 development has focused largely on eliciting neutralizing antibodies against the S protein to inhibit  
68 infection and reduce disease severity,<sup>10-14</sup> however, S-specific T-cell responses have been reported  
69 for two available vaccines, mRNA1273 and BNT162b1.<sup>15,16</sup>

70 SARS-CoV-2 strain analysis in participants in Phase 3 studies in South Africa has revealed  
71 that some vaccines show diminished protection against the B.1.351 variant strain,<sup>17</sup> including  
72 ChAdOx,<sup>18</sup> NVX-CoV2373,<sup>19,20</sup> and Ad26.COV2-S.<sup>21</sup> In addition, *in vitro* studies show that wild  
73 type S-specific antibodies elicited by mRNA-1273 and BNT162b1 show reduced binding to the  
74 B.1.351 variant S protein.<sup>22-25</sup> Taken together, these findings raise the concern that monovalent

75 vaccines targeting only the S protein may not be an optimal strategy for conferring protection  
76 against continually emerging variants.

77 SARS-CoV-2 expresses a number of other immunogenic proteins that may induce protective  
78 antibody and/or T-cell responses. Among these, the N protein is the most abundantly expressed, is  
79 highly conserved among coronaviruses, and has been studied previously as an antigen for  
80 therapeutics and vaccines for SARS-CoV.<sup>26-30</sup> Inclusion of N-derived antigens into vaccine  
81 designs may be a rational strategy to elicit broader protective immunity against SARS-CoV-2 with  
82 a high probability of being sustained against variants. The N protein associates with viral RNA  
83 within the SARS-CoV-2 virion and is necessary for viral RNA replication, virion assembly, and  
84 release from host cells.<sup>29,30</sup> Virtually all SARS-CoV-2 convalescents develop N-specific antibody  
85 and CD8<sup>+</sup> and/or CD4<sup>+</sup> T-cell responses.<sup>31</sup> SARS-CoV convalescents from 2003 maintain robust  
86 cognate N-specific CD8<sup>+</sup> and/or CD4<sup>+</sup> T-cell responses that were detectable up to 17 years later.<sup>32</sup>  
87 These long-lived memory T cells also cross-react with N and other proteins of SARS-CoV-2.<sup>32</sup>  
88 To a lesser extent, individuals with no history of exposure to SARS-CoV, SARS-CoV-2, or Middle  
89 Eastern Respiratory Syndrome (MERS) also show cross-reactive SARS-CoV-2 N-specific CD8<sup>+</sup>  
90 and/or CD4<sup>+</sup> T-cell responses, likely due to prior exposure to related endemic coronaviruses  
91 including OC43, HKU1, 229E, and NL63.<sup>31</sup> These data suggest that induction of N-specific  
92 memory T-cell responses via vaccination may at least partly recapitulate the natural course of  
93 SARS-CoV-2 infection and recovery from illness, and could be beneficial for achieving more  
94 optimal disease-limiting immunity against the virus.

95 Recent characterization of COVID-19 patient immune responses to SARS-CoV-2 indicates  
96 T-cell activation is critical for clearance of infection and production of long-term immunity to  
97 coronavirus infections.<sup>32-35</sup> Both CD4<sup>+</sup> and CD8<sup>+</sup> T cells underpin durable immune responses  
98 because CD4<sup>+</sup> T cells, while not effector cells like CD8<sup>+</sup> T cells, are critical to the generation of

99 robust and long-lasting immunity afforded by antibody-secreting plasma cells and the elimination  
100 of infected cells by memory cytotoxic CD8<sup>+</sup> T cells.<sup>36,37</sup>

101 Here, to support our hypothesis that a vaccine that generates vigorous T-cell responses has a  
102 reasonable likelihood of sustaining efficacy against emerging variants, we first describe our *in*  
103 *silico* identification of 9-mer T-cell epitopes and prediction of HLA binding for both first-wave  
104 ‘A’ strain SARS-CoV-2 and the variants that are found in the B.1.351 strain discovered in South  
105 Africa – spike K417N, E484K, and N501Y and nucleocapsid T205I.

106 We then demonstrate that the hAd5 S-Fusion + N-ETSD (hAd5 S + N) COVID-19 vaccine  
107 antigens, when expressed by monocyte-derived dendritic cells (MoDCs) from individuals  
108 previously infected with SARS-CoV-2, can activate and induce recall of S- and N-specific  
109 autologous CD8<sup>+</sup> and CD4<sup>+</sup> T cells. Overall, N-ETSD was found to elicit greater T-cell responses  
110 than N without the ETSD. This study demonstrates the vaccine-expressed antigens are ‘recalled’  
111 by T cells and thus suggests they have the potential to induce relevant, protective immune  
112 responses in previously SARS-CoV-2 infected or vaccinated individuals who receive the hAd5 S  
113 + N vaccine.

114 We further report that T cells isolated 14 and 23 days after prime vaccination alone from  
115 participants in our ongoing Phase 1b clinical trials of the hAd5 S + N vaccine are activated by both  
116 S and N peptides pools and that these T-cell responses are not only comparable in magnitude to  
117 those of T cells from previously SARS-CoV-2 infected patients, activation by S peptides is  
118 sustained for variant S peptides, including those found in the B.1.1.7, B.1.429, P.1 and B.1.351  
119 strains.

## 120 **MATERIALS and METHODS**

### 121 ***In silico* T-Cell Epitope HLA Binding Prediction**

#### 122 *SARS-CoV-2 reference sequences*

123 The reference strain and COVID19 variants used for epitope analysis was assembled from  
124 75,000 individual sequences deposited in the GISAID database. Binding analysis was run on the  
125 consensus sequence generated using our in-house binding algorithm.<sup>38</sup> Briefly, neural network  
126 classifiers that process full HLA protein and query peptide amino acid sequences were trained on  
127 experimental binding data deposited in the IEDB database.<sup>39</sup> A classifier ensemble was leveraged  
128 to abstain from making predictions when output uncertainty overlapped the decision threshold,  
129 thus boosting robustness and precision of binding prediction results.

130 The variants assessed included (name/mutation(s)): B.1.1.7/A222V mutation; B.1.1.7/N501Y  
131 mutation; B.1.351 and B.1.1.28/K417N (or K417T for B.1.1.28), E484K, and the N501Y  
132 mutations; and P.1/E484K. Binding efficiencies as well as HLA-epitope pairs were compared  
133 between reference sequences and mutations to determine potential immune evasion due to the  
134 reported variants.

### 135 **Production of hAd5 S + N and related SARS-CoV-2 antigen expressing vectors.**

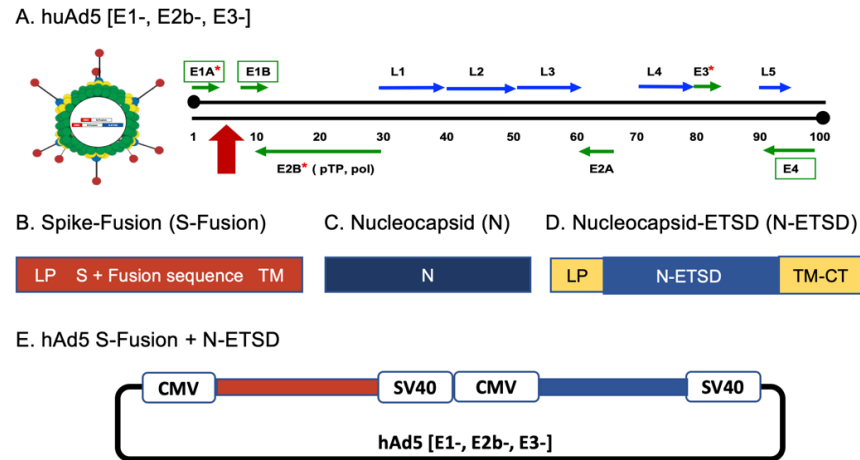
136 Production of all hAd5 [E1-, E2b-, E3-] (Fig. 1A) constructs and virus particles were carried  
137 out as previously described.<sup>40</sup> In brief, high titer adenoviral stocks were generated by serial  
138 propagation in the E1- and E2b-expressing E.C7 packaging cell line, followed by CsCl<sub>2</sub>  
139 purification, and dialysis into storage buffer (2.5% glycerol, 20 mM Tris pH 8, 25 mM NaCl) by  
140 ViraQuest Inc. (North Liberty, IA). Viral particle counts were determined by sodium dodecyl  
141 sulfate disruption and spectrophotometry at 260 and 280 nm. Viral titers were determined using  
142 the Adeno-X™ Rapid Titer Kit (Takara Bio).

143 The constructs created included:

144 Fig. 1B. S-Fusion: S optimized to enhance surface expression and display of RBD.

145 Fig. 1C. N (N without ETSD): Nucleocapsid (wild type) sequences with tags for immune detection,  
146 but without ETSD modification, and predominantly cytoplasmic localization.

147 Fig. 1D. N with the Enhanced T-cell Stimulation Domain (N-ETSD): Nucleocapsid (wild type)  
 148 with ETSD to direct endo/lysosomal localization and tags for immune detection.  
 149 Fig. 1E. The dual-antigen hAd5 S-Fusion + N-ETSD vaccine.



150  
 151 **Fig. 1** Human adenovirus serotype 5 (*hAd5*) platform and constructs. (A) *hAd5* with E1, E2b and  
 152 E3 regions deleted (*hAd5*[E1-, E2b-, E3-]). The site of antigen sequence insertion is shown with a  
 153 red arrow. Constructs tested included (B) spike (S)-Fusion, (C) nucleocapsid (N) without the  
 154 Enhanced T-cell Stimulation Domain (ETSD), (D) N-ETSD, and (E) the *hAd5* S-Fusion + N-  
 155 ETSD vaccine.

156  
 157 **The T-cell recall studies of unexposed and previously SARS-CoV-2 infected individuals**

158 *Collection of plasma and PBMCs for differentiation of MoDCs from patients with confirmed*  
 159 *previous SARS-CoV-2 infection and from virus-naïve volunteers*

160 Blood was collected with informed consent via venipuncture from volunteer patients (Pt) who  
 161 had either not been exposed (UNEX) to SARS-CoV-2 as confirmed by ELISA and multiple  
 162 negative SARS-CoV-2 tests or who had recovered from COVID-19 as indicated by recent medical  
 163 history and a positive SARS-CoV-2 antibody test. The presence of anti-S IgG and of neutralizing  
 164 antibodies in plasma from previously SARS-CoV-2 infected patients was confirmed by ELISA, a  
 165 surrogate neutralization assay,<sup>41</sup> and a live virus assay as shown in Supplementary Fig. S1. A third  
 166 source of whole blood was apheresis of healthy subjects from a commercial source (HemaCare).

167 Peripheral blood mononuclear cells (PBMCs) were isolated from whole blood by density  
 168 gradient centrifugation and plasma was collected after density gradient centrifugation.

169 Monocyte-derived dendritic cells (MoDC) were differentiated from PBMC using GM-CSF  
170 (200U/ml) and IL-4 (100U/ml) as previously described<sup>42</sup>. Briefly, monocytes were enriched by  
171 adherence on plastic, while the non-adherent cells were saved and frozen as a source of  
172 lymphocytes, specifically T cells. Adherent cells were differentiated into dendritic cells (3-5 d in  
173 RPMI containing 10% FBS), then frozen in liquid nitrogen for later use. T cells were enriched  
174 from the non-adherent fraction of PBMC using MojoSort (BioLegend CD3 enrichment). CD4+  
175 and CD8+ T cells were enriched using analogous kits from the same manufacturer. Efficiency of  
176 the cell separations was evaluated by flow cytometry.

177 *Transduction of MoDCs with hAd5 N-WT or N-ETSD and labeling with anti-N, anti-CD71, anti-*  
178 *LAMP-1, and Anti-LC3a/b antibodies*

179 Freshly thawed MoDCs were plated on 4-well Lab-Tek II CC2 Chamber Slides, using 3 x10<sup>4</sup>  
180 cells per well and transduction performed at MOI 5000 one hour after plating using hAd5 N-ETSD  
181 or hAd5 N. Slides were incubated o/n at 37°C, fixed in 4% paraformaldehyde for 15 minutes, then  
182 permeabilized with 1% Triton X100, in PBS) for 15 min. at room temperature. To label N, cells  
183 were then incubated with an anti-flag monoclonal (Anti-Flag M2 produced in mouse) antibody at  
184 1:1000 in phosphate buffered saline (PBS) with 3% BSA, 0.5% Triton X100 and 0.01% saponin  
185 overnight at 4°C, followed by three washes in PBS and a 1 hour incubation with a goat anti-Mouse  
186 IgG (H+L) Highly Cross-Adsorbed Secondary Antibody, Alexa Fluor Plus 555 (Life  
187 Technologies) at 1:500. For co-localization studies, cells were also incubated overnight at 4°C with  
188 a rabbit anti-CD71 (transferrin receptor, recycling/sorting endosomal marker) antibody  
189 (ThermoFisher) at 1:200; sheep anti-Lamp1 Alexa Fluor 488-conjugated (lysosomal marker)  
190 antibody (R&D systems) at 1:10; or a rabbit monoclonal anti human LC3a/b (Light Chain 3,  
191 autophagy marker) antibody (Cell Signaling Tech #12741S) used at 1:100. After removal of the  
192 primary antibody, two washes in PBS and three washes in PBS with 3% BSA, cells were incubated  
193 with fluor-conjugated secondary antibodies when applicable at 1:500 (Goat anti-Rabbit IgG (H+L)



194 secondary antibody, Alexa Fluor 488; 1:500 dilution) for 1 hour at room temperature. After brief  
195 washing, cells were mounted with Vectashield Antifade mounting medium with DAPI (Fisher  
196 Scientific) and immediately imaged using a Keyence all-in-one Fluorescence microscope camera  
197 and Keyence software.

198 *CD3<sup>+</sup> T-cell and selected CD4<sup>+</sup> and CD8<sup>+</sup> T-cell secretion of IFN- $\gamma$  in response to MoDCs*  
199 *pulsed with SARS-CoV-2 peptide antigen pools*

200 The ability of T cells from previously infected patients used in these studies to recognize  
201 SARS-CoV-2 antigens *in vitro* was validated and then similar analyses were performed for  
202 selected CD4<sup>+</sup> and CD8<sup>+</sup> T cells. Briefly, MoDC (2 x 10<sup>4</sup>) were pulsed with SARS-CoV-2 peptide  
203 antigens (1 $\mu$ g/ml, PepMix S comprising the S1 and S2 pools PM-WCPV-S-1; and N PM-WCPV-  
204 NCAP-1, both JPT Peptide Technologies) then autologous T cells (1 x 10<sup>5</sup>), enriched from the  
205 non-adherent fraction of PBMC using MojoSort (BioLegend CD3 enrichment) were added in  
206 enriched RPMI (10% human AB serum). Cells were cultured in a microtiter plate (Millipore)  
207 containing an immobilized primary antibody to target IFN- $\gamma$ , overnight (37°C), then IFN- $\gamma$  spot  
208 forming cells enumerated by ELISpot. For ELISpot detection, after aspiration and washing to  
209 remove cells and media, IFN- $\gamma$  was detected by a secondary antibody to cytokine conjugated to  
210 biotin. A streptavidin/horseradish peroxidase conjugate was used detect the biotin-conjugated  
211 secondary antibody. The number of spots per well (1 x 10<sup>5</sup> cells), was counted using an ELISpot  
212 plate reader. IL-4 was measured by ELISpot using a kit (MabTech) with wells precoated with anti-  
213 IL-4 antibody and following the manufacturer's instructions. Remaining steps for IL-4 detection  
214 were identical to those for IFN- $\gamma$ , but with alkaline phosphatase detection rather than peroxidase.  
215 *Determination of previously SARS-CoV-2 infected patient-derived T-cell reactivity in response to*  
216 *autologous hAd5 vaccine-transduced MoDCs*

217 MoDCs were transduced with hAd5 S-Fusion, S-Fusion + N-ETSD, N-ETSD, N or GFP/Null  
218 constructs and incubated overnight at 37°C. The transduced MoDCs were cultured with CD3+,  
219 CD4+, or CD8+ T cells from the same individuals overnight. Antigen specific T-cell responses  
220 were enumerated using ELISpot as described above.

## 221 **Phase 1b Clinical Trial and Analyses**

### 222 *Vaccination of healthy adult subjects with hAd5 S + N.*

223 The current Good Manufacturing Practice (cGMP) vaccine used in the clinical trial was  
224 prepared using the generated high titer adenoviral stocks described above in *Production of hAd5*  
225 *S + N and related SARS-CoV-2 antigen expressing vectors.*

226 In a phase 1b, open-label study (QUILT 4.001 in adults volunteers conducted at Hoag  
227 Hospital in Orange County, California, USA; the hAd5 S + N vaccine was administered  
228 subcutaneously (SC) at a dosage of  $1 \times 10^{11}$  VP to cohort 2 participants.

229 Study participants comprised healthy adult volunteers between the ages of 18 and 55. Subjects  
230 were assigned to cohorts. Data from cohort 2 (high dose) is presented here. All the participants  
231 provided informed, written consent before enrollment.

### 232 *Trial Oversight*

233 The trial protocol was approved by the Western IRB for the Chan Soon-Shiong Institute for  
234 Medicine (CSSIFM) and the Hoag Hospital Providence IRB at Hoag Hospital Newport Beach.  
235 ImmunityBio, Inc. was the regulatory sponsor of the trial and holder of the Investigational New  
236 Drug (IND) application. The trial was funded by ImmunityBio, Inc. The vaccine was designed and  
237 manufactured by ImmunityBio. *The studies presented here are experimental and all assays and*  
238 *analyses were performed in-house at ImmunityBio, Inc. Formal analyses of the primary and*  
239 *secondary end points are not reported in this manuscript.*

### 240 *T-cell analyses*

241 T-cell responses in PBMCs were measured at baseline (Day 1) and after prime vaccination  
242 alone on Day 14-16 and 21-23 by ELISpot for secretion of interferon  $\gamma$  (IFN $\gamma$ ) and interleukin 4  
243 (IFN-4). T helper cell type 1 dominance was determined based on the IFN $\gamma$ /IL-4 ratio.

#### 244 *IFN- $\gamma$ ELISpot for enumeration of S- and N-specific T cells in PBMC*

245 ELISpot assays were used to enumerate S- and N-specific IFN- $\gamma$ -secreting T cells in fresh  
246 PBMCs isolated from the blood of subjects vaccinated with hAd5 S + N. Whole blood was  
247 collected by venipuncture pre- and post-vaccination. PBMCs were isolated from whole blood by  
248 standard density gradient centrifugation and frozen in liquid nitrogen until use. On the day of assay,  
249 PBMCs were thawed and re-suspended in RPMI 10% human AB serum, then incubated with 2.5  
250  $\mu$ g/ml of SARS-CoV-2 S or N peptide pools (JPT Peptide Technologies catalogue # PM-WCPV-  
251 S and PM-WCPV-NCAP-1, respectively). Internal positive controls were incubated with 2.5  $\mu$ g/ml  
252 of CEFT peptide pool consisting of epitopes derived from human Cytomegalovirus, Epstein-Barr  
253 virus, Influenza A, and Clostridium tetani (JPT Peptide Technologies catalogue # PM-CEFT-4).  
254 Positive assay controls were incubated with a CD3/CD28/CD2 agonist (StemCell Technologies  
255 catalogue # 10970). Negative controls were incubated with media alone or 2  $\mu$ g/ml of SARS-CoV-  
256 2 membrane peptide pool (JPT Peptide Technologies catalogue # PM-WCPV-VME). The number  
257 of spot-forming cells (SFCs) per well ( $2.5-4 \times 10^5$  PBMCs) were enumerated using an ELISpot  
258 plate reader (Cellular Technologies Limited model # S6UNIV-01-7115). All IFN- $\gamma$  ELISpot  
259 reagents were obtained from a commercial kit and used according to manufacturer protocol  
260 (Cellular Technologies Limited catalogue # Hu IFN-g/IL-4).

#### 261 *Variant S peptides*

262 For the assessment of PBMC responses to variant S peptides, ELISpot assays were performed  
263 as described above using peptide mixes from JPT. Each mix comprised 315 peptides delivered in  
264 2 subpools of 158 and 157 peptides derived from a peptide scan through the entire spike

265 glycoprotein of SARS-CoV-2. The mixes included: PepMix™ SARS-CoV-2 lineage B.1.1.7  
266 (United Kingdom; PM-SARS2-SMUT01-1) covering the following mutations: H0069-, V0070-,  
267 Y0144-, N0501Y, A0570D, D0614G, P0681H, T0716I, S0982A, D1118H; PepMix™ SARS-  
268 CoV-2 lineage B.1.351 (South Africa; PM-SARS2-SMUT02-1) covering the following mutations:  
269 D0080A, D0215G, L0242-, A0243-, L0244-, K0417N, E0484K, N0501Y, D614G, A0701V;  
270 PepMix™ SARS-CoV-2 lineage P.1 (Brazil; PM-SARS2-SMUT03-1) covering the following  
271 mutations: L0018F, T0020N, P0026S, D0138Y, R0190S, K0417T, E0484K, N0501Y, D0614G,  
272 H0655Y, T1027I, V1176F; and PepMix™ SARS-CoV-2 lineage B.1.429 (Los Angeles; PM-  
273 SARS2-SMUT04-1) covering the following mutations: S0013I, W0152C, L0452R, D0614G.

## 274 **RESULTS**

### 275 **T-cell epitope HLA binding prediction**

#### 276 *In silico identification of 9-mer T-cell epitopes and HLA binding prediction suggests such* 277 *binding is not significantly affected by B.1.351 strain variants*

278 To understand and predict the possible effects emerging SARS-CoV-2 variants may have on  
279 vaccine-elicited T-cell protection, we utilized our in-house T-cell epitope identification and  
280 binding analysis pipeline to compare the first wave ‘A’ strain epitopes to the B.1.351 variant strain.

281 *In silico* epitope analysis of the reference strain assembled from 75,000 individual sequences  
282 deposited in the GISAID database <sup>43,52</sup> revealed 2479 MHC class I and 20963 MHC class II  
283 potential binders. Altogether, the SARS-CoV-2 variants (K417N, E484K and N501Y mutations)  
284 of the B.1.351 strain generate 10970 MHC class I and 18017 MHC class II unique epitopes.

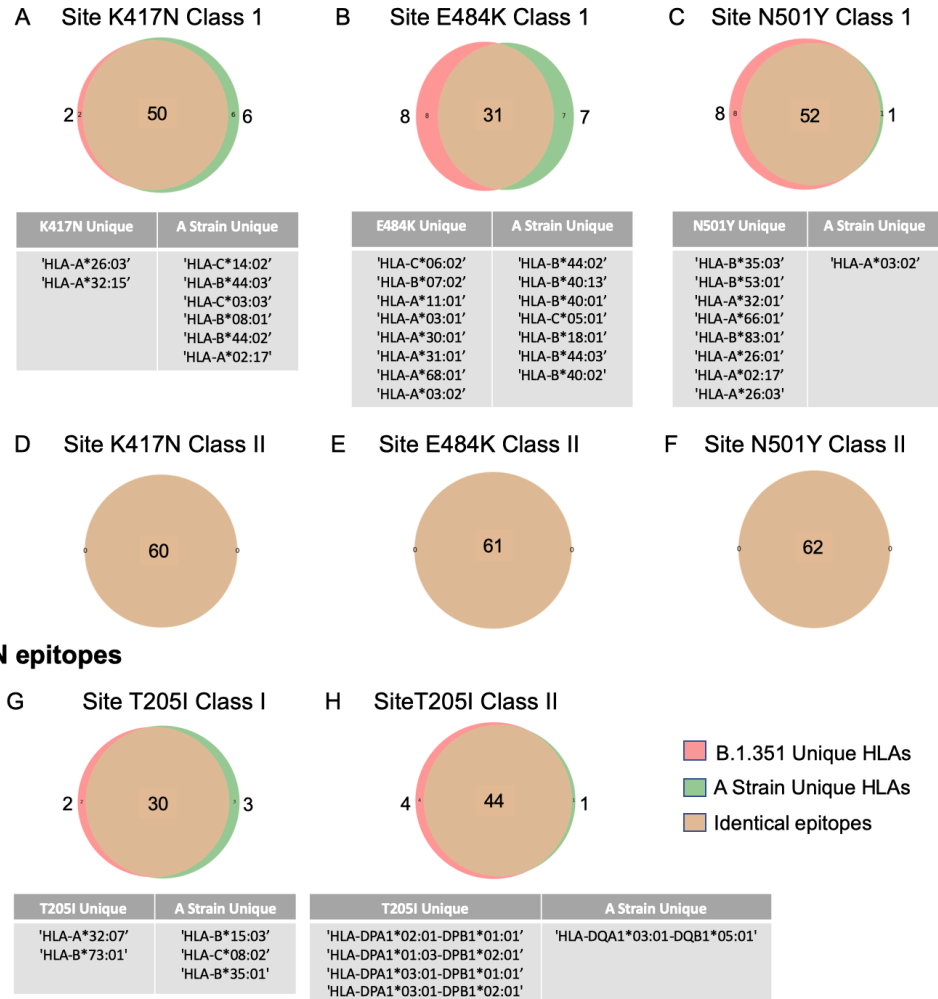
285 We compared these unique epitopes to the reference strain and counted the different epitopes  
286 that are bound by HLAs, finding 1659 unique MHC class I and 2887 unique MHC class II epitopes  
287 that only exist in the variants and not the original strain. These epitopes are from the S, envelope  
288 (E), N and membrane (M) proteins, but the most unique epitopes were found in variant S due to  
289 the higher numbers of coding mutations.

290 For HLA binding prediction, sequences and predicted binding were compared and aligned,  
291 and we found that, for example, as compared to the ‘A’ strain, a B.1.351 sequence has a 3 amino  
292 acid deletion that results in a unique sequence RFQTLHRSYL predicted to bind HLA-C\*14:02.  
293 By similar determination of the epitopes and HLAs from the reference strain and the B.1.351  
294 variants, differences were identified in binding affinity or HLAs. Similarly at the N501Y site, the  
295 reference strain generates an epitope (TNGVGYQPY) predicted to bind HLA-A\*30:02, while  
296 N501Y would generate a different yet similar epitope (TYGVGYQPY) also predicted to bind  
297 HLA-A\*30:02.

298 The key questions asked here were: how does mutation change HLA availability and which  
299 mutations favor immune evasion? Not all mutations lead to evasion; while a mutation may lead to  
300 an amino acid substitution that has potential functional consequences, that same mutation may still  
301 generate an epitope that retains HLA binding affinity and does not contribute to escape. The unique  
302 binding HLAs for each B.1.351 S variant when compared to the A strain are shown in Figure 2.  
303 For class I, for K417N there are only 2 unique HLAs and for the A strain there are 6 (Fig. 2A); for  
304 E484K there are 8 unique HLAs and for the A strain 7 (Fig. 2B); and for N501Y there are 8 unique  
305 HLAs and for the A strain only 1 (Fig. 2C). There are no unique class II HLAs for these same  
306 comparisons (Fig. 2D-F).

307 In the B.1.351 strain, there is only one N mutation – T205I. Similarly to the S variants, there  
308 are few unique binding HLAs. For class I, the T205I mutation generates 2 and the A strain 3 unique  
309 binding HLAs (Fig. 2G). For class II, the T205I generates 4 and the A strain just 1 unique binding  
310 HLA(s) (Fig. 2H).

## S epitopes



311  
 312 **Fig. 2** A high degree of overlap is seen for HLA binding of predicted T-cell epitopes from variants  
 313 and the first-wave A strain SARS-CoV-2. Comparison of 'A' and B.1.351 strain predicted class I  
 314 T-cell epitopes reveals significant overlap for the spike (A) K417N (50 of 58 epitopes), (B) E484K  
 315 (31 of 46 epitopes), and (C) N501Y (52 of 61 epitopes) variants. (D-F) Complete overlap is seen  
 316 for class II epitopes for those variants, respectively. (G) For T205I class I, 30 of 35 epitopes overlap  
 317 and (H) for class II, 44 of 49. Unique HLA class I binding is shown in the tables.  
 318

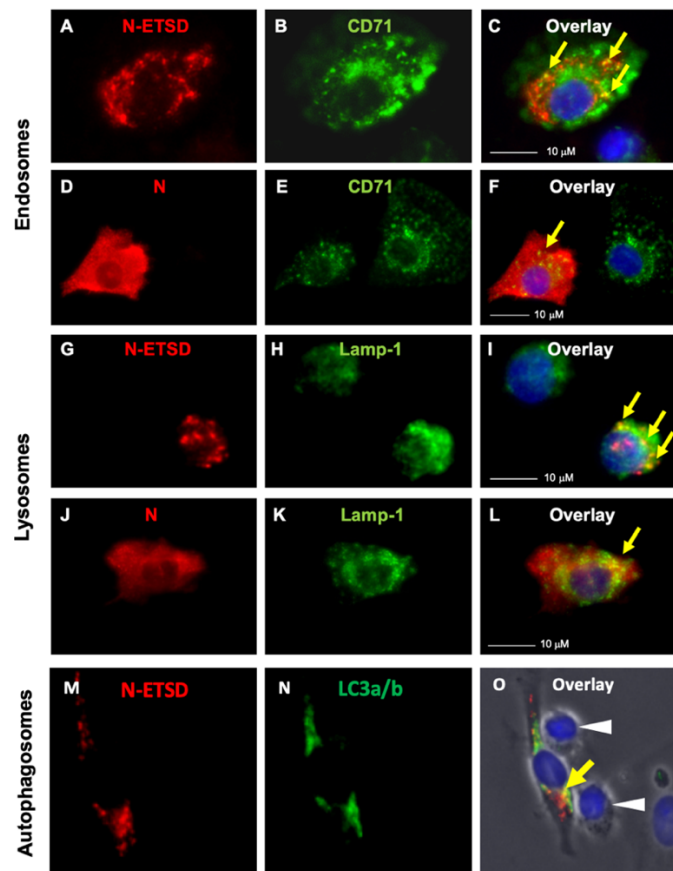
## 319 N-ETSD is directed to endo/lysosomal and autophagosomal compartments

320 The hAd5 dual antigen vaccine construct includes sequences designed to target N to MHC  
 321 class I and II antigen loading compartments (endo/lysosomes) to enhance T-cell responses.  
 322 Wildtype S is a surface-expressed protein, therefore the addition of a targeting sequence is not  
 323 necessary. To confirm N-ETSD is directed to endo/lysosomes, we evaluated the localization of N-  
 324 ETSD in human monocyte-derived dendritic cells (MoDCs) compared to its untargeted

325 cytoplasmic counterpart (N). MoDCs from healthy subjects were infected with hAd5 N-ETSD or  
326 hAd5 N and localization was determined by immunocytochemistry. N-ETSD showed localization  
327 to discrete vesicles, some coincident with CD71, a marker of recycling endosomes (Fig. 3A-C),  
328 and LAMP-1, a marker for late endosomes/lysosomes (Fig. 3G-I), whereas untargeted N was  
329 expressed diffusely and uniformly throughout the cytoplasm (Fig. 3D-F; J-L).

330 Studies have shown that lysosomes fuse with autophagosomes to enhance peptide processing  
331 and MHC class II presentation.<sup>44,45</sup> Thus we examined whether N-ETSD localized in  
332 autophagosomes in MoDCs by co-labeling with the autophagosome marker LC3a/b<sup>46</sup> to identify  
333 another potential site of localization relevant to MHC class II antigen presentation.<sup>47</sup> We found  
334 that N-ETSD also displayed some co-localization with the autophagosome marker (Fig. 3M-O).

335 Protein processing in autophagosomes plays a key role in MHC-mediated antigen presentation  
336 in DCs,<sup>48-50</sup> providing a potential mechanism of enhanced CD4+ T cells induced by N-ETSD in  
337 the vaccine construct. Evidence of this T-cell interaction with a MoDC infected with N-ETSD  
338 translocated to autophagosomes (and, it is assumed, also endosomes and lysosomes) is seen in this  
339 phase-contrast microscopy of the N-ETSD and LC3a/b co-labeled cells, which reveals the  
340 elongated DC morphology in contrast to the spherical morphology of what are posited to be  
341 undifferentiated lymphocytes.



342  
343 **Fig. 3** *N-ETSD localizes to endosomes, lysosomes, and autophagosomes.* MoDCs were infected  
344 with Ad5 N-ETSD or N without ETSD and were co-labeled with anti-flag (N, N-ETSD here have  
345 a flag tag) and anti-CD71 (endosomal marker), anti-Lamp 1 (lysosomal marker), or anti-LC3a/b  
346 antibodies. (A) N-ETSD, (B) CD71, and (C) overlay. (D) N, (E) CD71, and (F) overlay. (G) N-  
347 ETSD, (H) Lamp-1, and (I) overlay. (J) N, (K) Lamp-1, and (L) overlay. (M) N-ETSD, (N)  
348 LC3a/b, and (O) overlay. N/N-ETSD is red, other markers green, co-localization indicated by  
349 yellow arrows, and white arrows indicate suspected undifferentiated lymphocytes.

350

### 351 **T-Cell memory in patients previously infected with SARS-CoV-2**

#### 352 *Blood samples from previously SARS-CoV-2 infected patients show antibody and T-cell* 353 *responses and enhanced binding to hAd5 S + N expressing cells*

354 For the ‘recall’ studies described below, plasma samples were collected from four individuals  
355 convalescing from SARS-CoV-2 infection as confirmed by antibody assays and patient history.  
356 The presence of anti-Spike IgG, and neutralizing antibodies by both a surrogate SARS-CoV-2  
357 neutralization<sup>41</sup> and live virus assays, were confirmed in all patient samples (Supplementary Fig.  
358 S1). Samples from four virus-naïve individuals were used as controls.



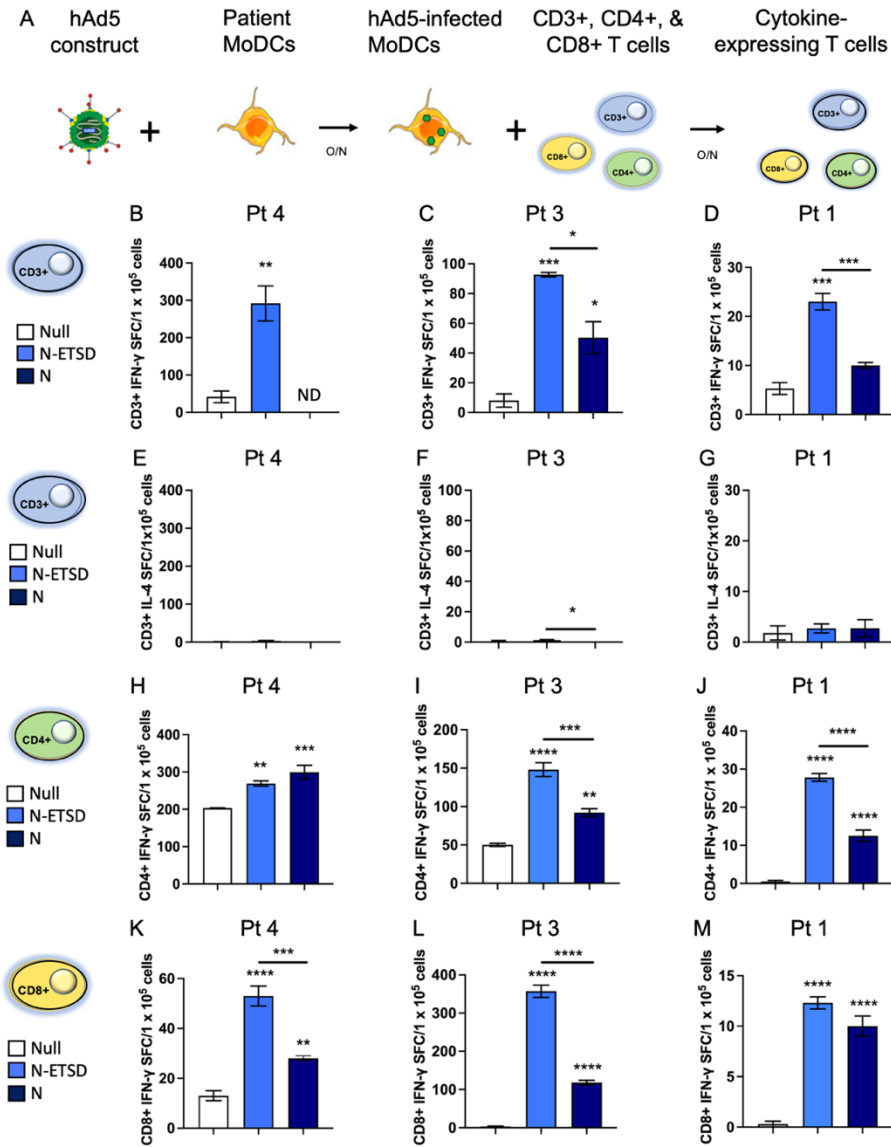
359 In additional studies to validate immune responses to SARS-CoV-2 antigens, the binding of  
360 previously SARS-CoV-2 infected patient and virus-naïve control individual plasma to human  
361 embryonic kidney (HEK) 293T cells transfected with either hAd5 S-Fusion alone or hAd5 S + N  
362 was assessed (Supplementary Fig. S2). This binding reflects the presence of antibodies in plasma  
363 that recognize antigens expressed by the hAd5 vectored vaccines. Quantification of histograms  
364 showed little or no binding of virus-naïve plasma antibodies to cells expressing constructs, with  
365 the highest previously SARS-CoV-2 infected patient plasma binding to cells expressing the dual  
366 antigen S-Fusion + N-ETSD construct (Supplementary Fig. S2R).

367 To confirm the T cells from previously SARS-CoV-2-infected patients were reactive to  
368 SARS-CoV-2 peptides, isolated T cells from the patients were incubated with S1 (containing the  
369 S receptor binding domain), S2 and N peptides pools. T cells from all four patients showed  
370 reactivity (Supplementary Fig. S3). Selected CD4+ and CD8+ T cells from 2 patients were  
371 activated by S1, S2, and N peptides, revealing CD8+ T cells were more reactive to N  
372 (Supplementary Fig. S3D and E).

373 ***Previously SARS-CoV-2 infected patient Th1 dominant CD3+ and CD4+/CD8+ memory T-cells***  
374 ***recall N-ETSD antigens expressed by autologous hAd5-infected MoDCs***

375 To evaluate the immune significance of endo/lysosome-localized N-ETSD versus cytoplasmic  
376 N, MoDCs were infected with hAd5 Null, N-ETSD or N constructs then incubated with autologous  
377 CD3+/-, or CD4+/-/CD8+-selected T cells (Fig. 4A). CD3+ T cells from previously infected SARS-  
378 CoV-2 patients showed significantly greater IFN- $\gamma$  secretion in response to N-ETSD than both  
379 Null and cytoplasmic N in the two patients (Pt 3 and Pt 1) where N-ETSD and N were compared  
380 (Fig. 4F and J). Interleukin-4 (IL-4) secretion by CD3+ T cells was low for all patients (Fig. 4C,  
381 G, and K); high IFN- $\gamma$  and low IL-4 responses show Th1 dominance for both N-ETSD and N. Both  
382 CD4+ and CD8+ selected T-cell populations showed significantly greater IFN- $\gamma$  responses to N-

383 ETSD than Null (Fig. 4D, E H, I, L and M) and in two of three patients, CD4+ and CD8+ T cells  
 384 showed greater recognition of N-ETSD compared to N.



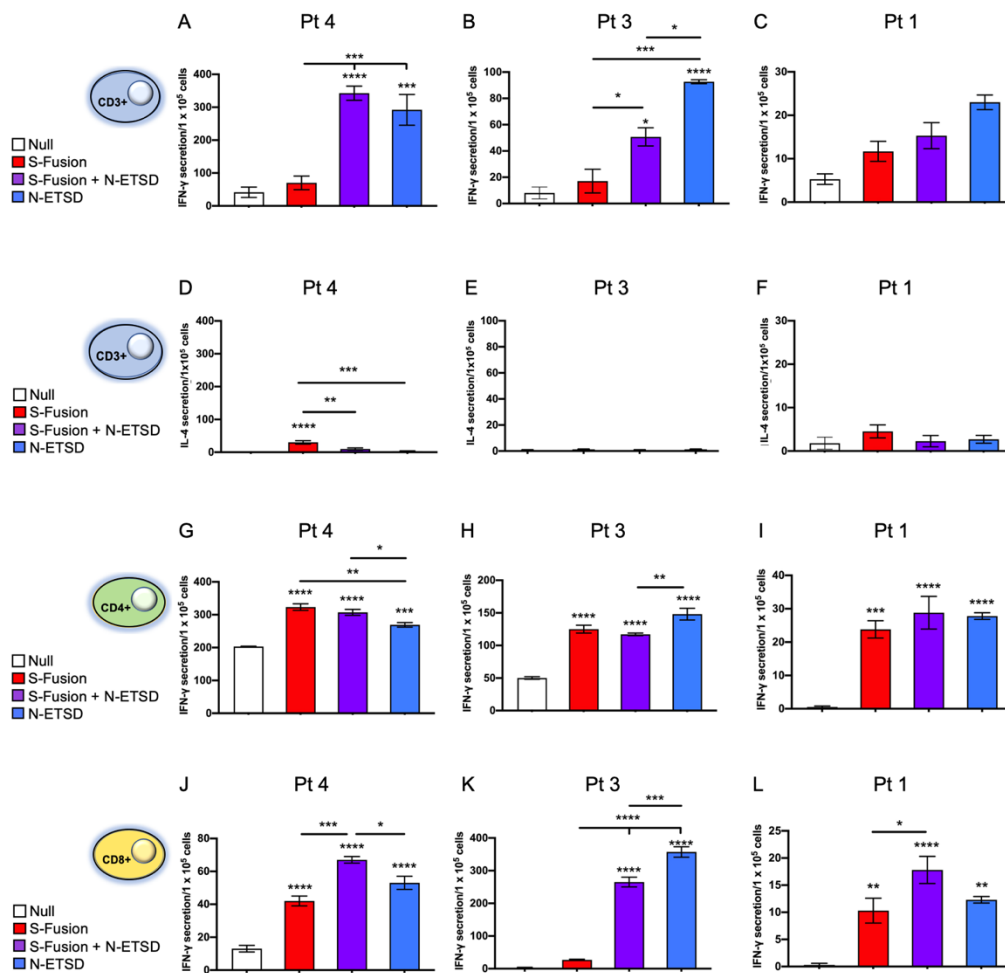
385  
 386 **Fig. 4** Previously SARS-CoV-2 infected patient T-cell IFN- $\gamma$  secretion is greater in response to  
 387 MoDC-expressed N-ETSD than N and is Th1 dominant. (A) Experimental design. (B-C) IFN- $\gamma$   
 388 and (D-F) secretion by autologous CD3+ T cells in response to hAd5 N-ETSD/N/Null-  
 389 expressing MoDCs for 3 previously infected patient. Same scale used for IFN- $\gamma$  and IL-4 for each  
 390 patient (B/E; C/F; D/G). IFN- $\gamma$  secretion by CD4+ (H-J) and CD8+ (K-M) T cells in response to  
 391 hAd5-N-ETSD/N/Null are shown. Statistical analysis performed using One-way ANOVA and  
 392 Tukey's post-hoc multiple comparison analysis, where \* $p$ <=0.05; \*\* $p$ <0.01, \*\*\* $p$ <0.001 and  
 393 \*\*\*\* $p$ <0.0001. Comparison to Null shown above bars, comparison between N-ETSD and N  
 394 indicated with a line. Data graphed as mean and SEM;  $n$  = 3-4.  
 395

396 *CD4+ and CD8+ memory T cells from previously SARS-CoV-2 infected patients recall*  
397 *nucleocapsid and spike antigens expressed by autologous hAd5-infected MoDCs*

398 To compare CD3+, CD4+, and CD8+ memory T-cell responses to the components of the hAd5  
399 S + N vaccine, MoDCs were infected with hAd5 S-Fusion, hAd5 N-ETSD, or the dual antigen  
400 vaccine (Fig. 5A).

401 For unselected CD3+ T cells, IFN- $\gamma$  responses were similar to S-Fusion + N-ETSD and N-  
402 ETSD with responses to S-Fusion being relatively low (Fig. 5A-C). The number of IL-4 secreting  
403 T cells in response to any infected MoDC was very low (Fig. 5D-F). Based on the increased  
404 expression of S in the dual antigen vaccine compared to monovalent S-Fusion, the increased T-  
405 cell responses could be explained by either T cells recognizing increased S or the presence of N.  
406 Importantly, these T-cell responses were characterized by a predominance of IFN- $\gamma$  (Th1) relative  
407 to IL-4 (Th2).

408 CD4+ T cells from all three patients showed significantly greater recognition of all three  
409 constructs compared to Null (Fig. 5G-I). While there were greater responses to specific constructs  
410 in some individuals, overall the responses to S-Fusion, S-Fusion + N-ETSD and N-ETSD were  
411 similar. CD8+ T cells from all three patients recognized the dual antigen and N-ETSD vaccines at  
412 a significantly higher level than Null; in only two of three patients did CD8+T cells recognize S-  
413 Fusion to a significant degree above Null (Fig. 5J-L). These data indicate that T cells from  
414 previously infected SARS-CoV-2 patients have reactivity and immune memory recall to both of  
415 the vaccine antigens (S and N) in our vaccine vector.



416  
 417 **Fig. 5** Previously SARS-CoV-2 infected patient T-cell responses to the dual antigen vaccine and  
 418 its individual components reveal distinct antigen specificity of T-cell populations. (A-C) CD3+ T  
 419 cell IFN- $\gamma$  responses for three patients. (D-F) CD3+ T cell IL-4 responses. (G-I) CD4+ IFN- $\gamma$   
 420 responses. (J-L) CD8+ IFN- $\gamma$  responses. Statistical analysis performed using One-way ANOVA  
 421 and Tukey's post-hoc multiple comparison analysis to compare each construct to the Null  
 422 construct, where \* $p < 0.05$ ; \*\* $p \leq 0.01$ ; \*\*\* $p \leq 0.001$ ; and \*\*\*\* $p \leq 0.00001$ . Comparison to Null  
 423 only above bars; comparison between antigen-expressing constructs above lines. Data graphed as  
 424 mean and SEM;  $n = 3-4$ .

425  
 426 **T-Cell Responses after a Single Prime Vaccination in a Phase 1 Clinical Trial**

427 For the ELISpot assay results shown here, T cells were isolated from patients in cohort 2 of  
 428 the Phase 1b study of the ImmunityBio hAd5 COVID-19 'T-cell' vaccine (NCT04591717). These  
 429 participants were vaccinated subcutaneously with  $1 \times 10^{11}$  hAd5 S + N viral particles (VP).

430 The studies presented here are experimental and all assays and analyses were performed in-  
 431 house at ImmunityBio, Inc. Formal analyses of the primary and secondary end points are ongoing  
 432 pending completion of the trial.

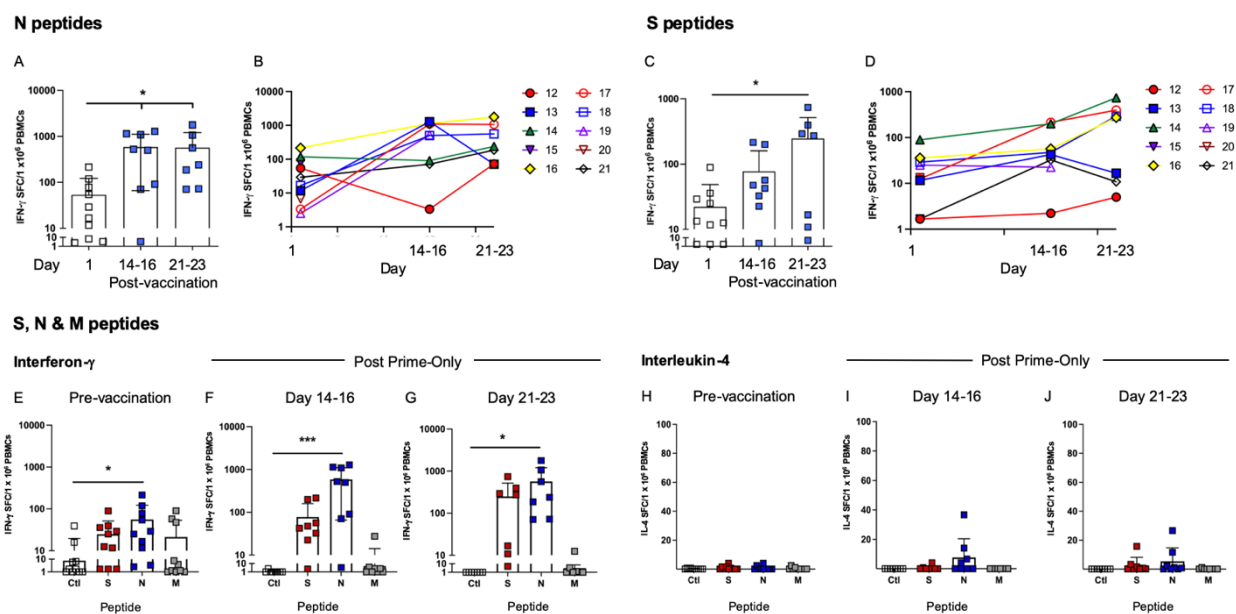
433 ***T cells from vaccinated participants show Th1 dominant responses to S and N by Day 14 after***  
434 ***a single prime injection, with a more than 10-fold increase in mean responses to N***

435 T-cell responses to S, N, and SARS-CoV-2 membrane (M) peptides were determined by  
436 ELISpot for clinical study participants pre-vaccination (Day 1) and at two time points following  
437 the prime injection: Days 14-16 and 21-23.

438 By Day 14-16, mean T-cell secretion of IFN- $\gamma$  in response to N peptides increased more than  
439 10-fold compared to pre-vaccination (Day 1); these responses were sustained on Day 21-23 and  
440 were significant (Fig. 6A). The changes in T-cell responses to N for individual participants from  
441 pre- to post-vaccination are shown in Fig. 6B.

442 T-cell secretion of IFN- $\gamma$  in response to S peptides also increased post-prime only vaccination,  
443 with the mean increasing more than 3-fold by Day 14-16 and more than 10-fold by Day 21-23,  
444 when differences were significant (Fig. 6C). T-cell responses to S for individual participants are  
445 shown in Fig. 6D.

446 When responses to S, N and SARS-CoV-2 membrane (M) peptides are compared, the greatest  
447 responses are seen to N peptides (Fig. 6F and G). As expected, there were very low/no responses  
448 to M peptide, not delivered in the vaccine. Importantly, IL-4 secretion in response to peptide  
449 stimulation was very low, indicating all responses to vaccine antigens were highly Th1 dominant.

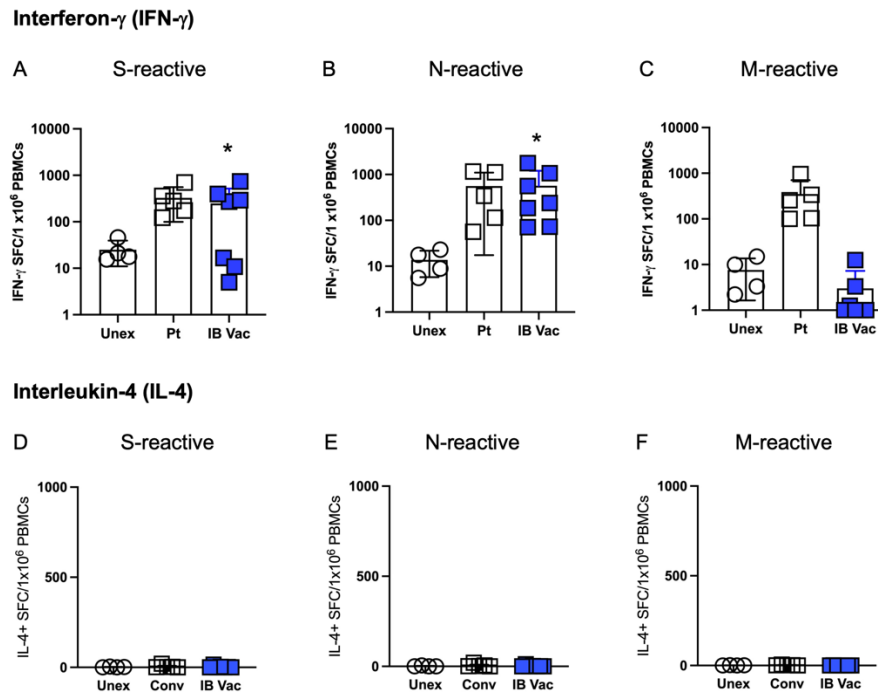


450  
 451 **Fig. 6** Vaccinated participant T-cell responses to S, N, and M peptides. (A) T-cell interferon- $\gamma$   
 452 (IFN- $\gamma$ ) secretion in response to nucleocapsid (N) peptides is shown for pre-vaccination (Day 1)  
 453 and post-prime only Day 14-16 and 21-23. (B) Individual participant T-cell responses to N. (C) T-  
 454 cell IFN- $\gamma$  secretion in response to spike (S) peptides is shown for pre-vaccination (Day 1) and  
 455 post-prime only Day 14-16 and 21-23. (D) Individual participant T-cell responses to S. T-cell IFN-  
 456  $\gamma$  secretion in response to no stimulation (Ctl), S, N and membrane (M): (E) pre-vaccination and  
 457 on (F) Day 14-16 and (G) 21-23 post-prime only; (H-J) interleukin-4 (IL-4) secretion. Statistical  
 458 analysis performed using One-way ANOVA and Sidak's post-hoc analysis to compare pre-to post-  
 459 vaccination (A, C) or peptide stimulation to Ctl (E-J), where \*p < 0.05, \*\*p  $\leq$  0.01, and \*\*\*p  $\leq$   
 460 0.001. Data graphed as mean and SD; baseline n = 9, Day 14-16 n = 7, Day 21-23 n = 7.

461  
 462 **T-cell responses to S and N antigens generated from hAd5 prime vaccination alone were**  
 463 **equivalent to those from previously SARS-CoV-2 infected patients**

464 As shown in Figure 7, T-cell responses to both N and S for previously SARS-CoV-2 infected  
 465 patients (Pt) and hAd5 S + N vaccinated participants (IB Vac) on Day 21-23 were comparable.  
 466 For responses to N, both Pt and IB Vac were ~40-fold greater than Unex; and for responses to S,  
 467 both Pt and IB Vac were >15-fold higher than Unex. As expected, T cells from previously SARS-  
 468 CoV-2 infected patients, but not vaccinated participants, reacted to M due to its presence in the  
 469 live virus. The M antigen is not present in the vaccine.

470

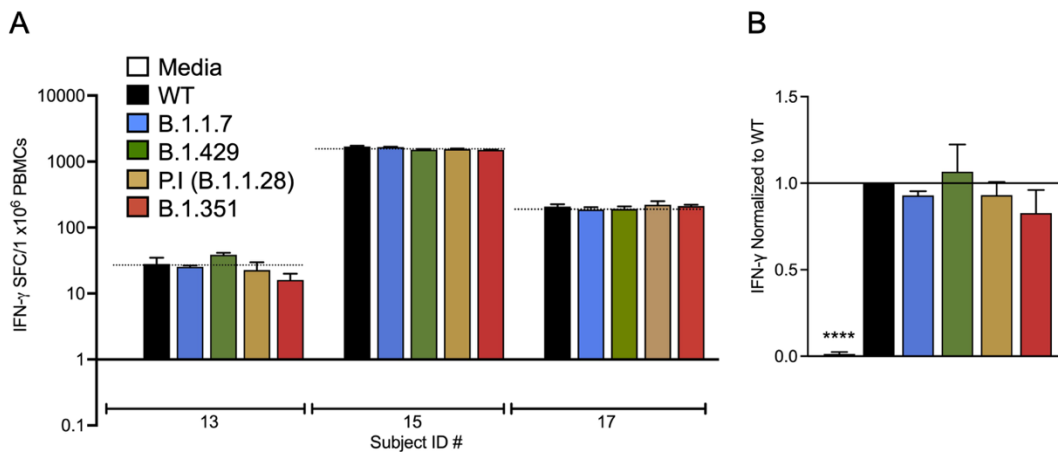


471  
 472 **Fig. 7** T-cells from vaccinated and previously SARS-CoV-2 infected individuals show similar  
 473 responses to S and N. T-cell secretion of interferon- $\gamma$  (IFN- $\gamma$ ) in response to (A) N, (B) S, and (C)  
 474 M as determined by ELISpot shown for SARS-CoV-2 unexposed (Unex) and previously infected  
 475 (Pt) individuals as compared to participants receiving a prime vaccination alone (IB Vac) from  
 476 Day 21-23. Secretion of interleukin-4 (IL-4) in response to (D) N, (E) S, and (F) M. Statistical  
 477 analysis performed using a Wilcoxon signed-rank test where \*p < 0.05. Data graphed as mean and  
 478 SEM; Unex n = 4, Pt n = 5, IB vac n = 7.

479  
 480 **T cells from hAd5 S + N vaccinated participants show equivalent reactivity to S wild type and**  
 481 **variant peptides**

482 To determine if vaccinated participant T-cell responses seen to S wildtype (WT) peptide pools  
 483 after only prime vaccination are sustained in response to S variant peptide pools, these responses  
 484 were assessed by ELISpot to pools comprising the variants B.1.1.7 (H0069 $\delta$ , V0070 $\delta$ , Y0144 $\delta$ ,  
 485 N0501Y, A0570D, D0614G, P0681H, T0716I, S0982A, and D1118H mutations), B.1.429  
 486 (S0013I, W0152C, L0452R, and D0614G mutations), P.1/B.1.1.28 clade (L0018F, T0020N,  
 487 P0026S, D0138Y, R0190S, K0417T, E0484K, N0501Y, D0614G, H0655Y, T1027I, and V1176F  
 488 mutations), and B.1.351 (D0080A, D0215G, L0242-, A0243-, L0244-, K0417N, E0484K,  
 489 N0501Y, D614G, and A0701V mutations).

490 As shown in Figure 8A, for all 3 vaccinated participants from which sufficient PBMCs were  
491 available for assessment, IFN- $\gamma$  secretion in response to the S WT sequence used in the hAd5 S +  
492 N vaccine and the mutant S peptide pools was very similar. When graphed together after  
493 normalization of T-cell IFN- $\gamma$  secretion in response to media/S variants to S WT (S WT = 1.0) for  
494 each individual, there are no statistical differences between responses to S WT and any variant,  
495 while the difference between media and S WT was highly significant.



496 **Fig. 8** T cells from vaccinated participants show similar responses to S wildtype (WT) and S  
497 variants. (A) T-cell secretion of interferon- $\gamma$  (IFN- $\gamma$ ) in response to medium only (media), S WT  
498 peptides or B.1.1.7 S, B.1.429, P.1 (B.1.1.28 clade), and B.1.351 variant peptides as determined  
499 by ELISpot is shown for 3 vaccinated participants after a single injection of the vaccine. (B) IFN-  
500  $\gamma$  secretion normalized to S WT for the 3 vaccinated participants combined. Statistical analysis  
501 performed using One-Way ANOVA with Dunnett's post-hoc analysis comparing media and  
502 variant peptide pools to the S-WT peptide pool, where \* $p < 0.05$  and \*\*\*\* $p \leq 0.0001$ ;  $n = 3$ . Data  
503 graphed as the mean plus SEM.  
504  
505

## 506 DISCUSSION

507 The emergence and rapid spread of SARS-CoV-2 variants is raising concern that first  
508 generation monovalent wild-type S-targeting vaccines may eventually show reduced protection  
509 against COVID-19. In addition to updating S sequences to include variants in current vaccines,  
510 alternate or complimentary vaccine strategies include enhanced focus on eliciting protective T-cell  
511 responses and addition of other immunogenic structural proteins, such as M and/or N. Evidence  
512 indicates that virtually all COVID-19 convalescents develop IFN- $\gamma$ -secreting CD4<sup>+</sup> and/or CD8<sup>+</sup>  
513 T-cell responses not only against S, but also against the M and N proteins of SARS-CoV-2. <sup>31</sup>



514 Significant T-cell reactivity in COVID-19 convalescents has also been observed against a wide  
515 breadth of other SARS-CoV-2 proteins, particularly nsp6 and ORF3a.<sup>28,31,51</sup> Collectively, the total  
516 magnitude of the T-cell response against non-S proteins such as N appears at least equal to or  
517 possibly greater than the T-cell response against S in COVID-19 convalescents.<sup>28,31,51</sup> These data  
518 suggest that T-cell responses (when present) elicited by monovalent S-targeting vaccines designed  
519 to generate humoral responses likely provide limited cell-mediated protection.

520 Here we show that our strategy of including N-ETSD, confirmed to be directed to the  
521 endo/lysosomal compartment with S optimized for cell-surface display<sup>1,52</sup> results in recognition  
522 of the N-ETSD and S-Fusion + N-ETSD antigen(s) by previously SARS-CoV-2 patient T cells  
523 and in generation of S- and N-reactive T cells in participants receiving the hAd5 S-Fusion + N-  
524 ETSD vaccine. The enhancement of T-cell responses by the addition of N in this vaccine confers  
525 a greater likelihood of sustained protection against variants as our T-cell epitope HLA binding  
526 prediction analysis suggests.

527 The report of Redd *et al.*<sup>7</sup> provides further support for the merits of T-cell protection against  
528 variants. In their study, the authors assessed reactivity of CD8+ T cells from thirty COVID-19  
529 convalescent individuals to forty-five different mutations and concluded that virtually all CD8+ T  
530 cell responses to SARS-CoV-2 antigens should recognize the variants. The data presented here  
531 align with their findings and provide evidence that the hAd5 S-Fusion + N-ETSD vaccine has the  
532 potential to provide cellular immunity against SARS-CoV-2 variants.

533 Our dual-antigen hAd5 S + N vaccine, which is predicted to provide expanded T-cell  
534 protection, may have utility as a ‘universal’ booster. Not only would boosting with this vaccine  
535 likely increase cell-mediated protection for individuals who have already received a first-  
536 generation S-only vaccine, because the N protein is highly conserved among coronaviruses,<sup>53</sup> the  
537 hAd5-S-Fusion + N-ETSD vaccine might provide protection against viruses similar to SARS-  
538 CoV-2 that may arise.

539 The hAd5 S-Fusion + N-ETSD COVID-19 T-cell vaccine is currently undergoing clinical  
540 testing with delivery by a variety of routes, including sublingual, SC, intranasal, and a thermally-  
541 stable oral tablet as a prime/boost to provide protection against SARS-CoV-2. We anticipate our  
542 testing its use as a universal boost for current first generation vaccines in the near future.

543

## 544 ACKNOWLEDGEMENTS

545 We thank the volunteers participating in our Phase I COVID-19 vaccine clinical trial and  
546 Deborah Fridman, Director of Clinical Research at Hoag Hospital (Irvine/Newport Beach, CA).  
547 We also thank Phil Yang of ImmunityBio for his ongoing coordination of project updates for the  
548 studies described herein.

549

## 550 REFERENCES

- 551 1 Gabitzsch, E. *et al.* Complete Protection of Nasal and Lung Airways Against SARS-  
552 CoV-2 Challenge by Antibody Plus Th1 Dominant N- and S-Specific T-Cell Responses  
553 to Subcutaneous Prime and Thermally-Stable Oral Boost Bivalent hAd5 Vaccination in  
554 an NHP Study. *bioRxiv* **2020.12.08.416297**, doi:10.1101/2020.12.08.416297 (2021).
- 555 2 Amalfitano, A. Next-generation adenoviral vectors: new and improved. *Gene Therapy* **6**,  
556 1643-1645, doi:10.1038/sj.gt.3301027 (1999).
- 557 3 Gabitzsch, E. S. & Jones, F. R. New recombinant SAd5 vector overcomes Ad5 immunity  
558 allowing for multiple safe, homologous, immunizations. *J Clin Cell Immunol* **S4**, 001,  
559 doi:10.4172/2155-9899 (2011).
- 560 4 Gabitzsch, E. S. *et al.* Anti-tumor immunotherapy despite immunity to adenovirus using a  
561 novel adenoviral vector Ad5 [E1-, E2b-]-CEA. *Cancer Immunology, Immunotherapy* **59**,  
562 1131-1135, doi:10.1007/s00262-010-0847-8 (2010).
- 563 5 Gatti-Mays, M. E. *et al.* A Phase I Trial Using a Multitargeted Recombinant Adenovirus  
564 5 (CEA/MUC1/Brachyury)-Based Immunotherapy Vaccine Regimen in Patients with  
565 Advanced Cancer. *Oncologist* **25**, 479, doi:10.1634/theoncologist.2019-0608 (2019).
- 566 6 Hellerstein, M. What are the roles of antibodies versus a durable, high quality T-cell  
567 response in protective immunity against SARS-CoV-2? *Vaccine X* **6**, 100076,  
568 doi:10.1016/j.jvacx.2020.100076 (2020).
- 569 7 Redd, A. D. *et al.* CD8+ T cell responses in COVID-19 convalescent individuals target  
570 conserved epitopes from multiple prominent SARS-CoV-2 circulating variants. *Open*  
571 *Forum Infect Dis*, doi:10.1093/ofid/ofab143 (2021).
- 572 8 NIH. T cells recognize recent SARS-CoV-2 variants. *News Release*  
573 [https://www.nih.gov/news-events/news-releases/t-cells-recognize-recent-sars-cov-2-](https://www.nih.gov/news-events/news-releases/t-cells-recognize-recent-sars-cov-2-variants)  
574 [variants](https://www.nih.gov/news-events/news-releases/t-cells-recognize-recent-sars-cov-2-variants) (2021).

- 575 9 Tarke, A. *et al.* Negligible impact of SARS-CoV-2 variants on CD4+ and CD8+ T cell  
576 reactivity in COVID-19 exposed donors and vaccinees. *bioRxiv* **2021.02.27.433180**,  
577 doi:10.1101/2021.02.27.433180 (2021).
- 578 10 Baden, L. R. *et al.* Efficacy and Safety of the mRNA-1273 SARS-CoV-2 Vaccine. *N*  
579 *Engl J Med* **384**, 403-416, doi:10.1056/NEJMoa2035389 (2021).
- 580 11 Polack, F. P. *et al.* Safety and Efficacy of the BNT162b2 mRNA Covid-19 Vaccine. *N*  
581 *Engl J Med* **383**, 2603-2615, doi:10.1056/NEJMoa2034577 (2020).
- 582 12 Sadoff, J. *et al.* Interim Results of a Phase 1-2a Trial of Ad26.COV2.S Covid-19  
583 Vaccine. *N Engl J Med* **384**, 1824-1835, doi:10.1056/NEJMoa2034201 (2021).
- 584 13 Ewer, K. J. *et al.* T cell and antibody responses induced by a single dose of ChAdOx1  
585 nCoV-19 (AZD1222) vaccine in a phase 1/2 clinical trial. *Nat Med* **27**, 270-278,  
586 doi:10.1038/s41591-020-01194-5 (2021).
- 587 14 Keech, C. *et al.* Phase 1-2 Trial of a SARS-CoV-2 Recombinant Spike Protein  
588 Nanoparticle Vaccine. *N Engl J Med* **383**, 2320-2332, doi:10.1056/NEJMoa2026920  
589 (2020).
- 590 15 Anderson, E. J. *et al.* Safety and Immunogenicity of SARS-CoV-2 mRNA-1273 Vaccine  
591 in Older Adults. *N Engl J Med* **383**, 2427-2438, doi:10.1056/NEJMoa2028436 (2020).
- 592 16 Sahin, U. *et al.* COVID-19 vaccine BNT162b1 elicits human antibody and T(H)1 T cell  
593 responses. *Nature* **586**, 594-599, doi:10.1038/s41586-020-2814-7 (2020).
- 594 17 Karim, S. S. A. Vaccines and SARS-CoV-2 variants: the urgent need for a correlate of  
595 protection. *Lancet* **397**, 1263-1264, doi:10.1016/S0140-6736(21)00468-2 (2021).
- 596 18 Madhi, S. A. *et al.* Efficacy of the ChAdOx1 nCoV-19 Covid-19 Vaccine against the  
597 B.1.351 Variant. *N Engl J Med* **384**, 1885-1898, doi:10.1056/NEJMoa2102214 (2021).
- 598 19 Novavax. Novavax COVID-19 Vaccine Demonstrates 89.3% Efficacy in UK Phase 3  
599 Trial. [https://ir.novavax.com/news-releases/news-release-details/novavax-covid-19-](https://ir.novavax.com/news-releases/news-release-details/novavax-covid-19-vaccine-demonstrates-893-efficacy-uk-phase-3)  
600 [vaccine-demonstrates-893-efficacy-uk-phase-3](https://ir.novavax.com/news-releases/news-release-details/novavax-covid-19-vaccine-demonstrates-893-efficacy-uk-phase-3) (2021).
- 601 20 Shinde, V. *et al.* Efficacy of NVX-CoV2373 Covid-19 Vaccine against the B.1.351  
602 Variant. *New England Journal of Medicine* **384**, 1899-1909,  
603 doi:10.1056/NEJMoa2103055 (2021).
- 604 21 Johnson & Johnson. Johnson & Johnson Announces Single-Shot Janssen COVID-19  
605 Vaccine Candidate Met Primary Endpoints in Interim Analysis of its Phase 3  
606 ENSEMBLE Trial. [https://www.janssen.com/johnson-johnson-announces-single-shot-](https://www.janssen.com/johnson-johnson-announces-single-shot-janssen-covid-19-vaccine-candidate-met-primary-endpoints)  
607 [janssen-covid-19-vaccine-candidate-met-primary-endpoints](https://www.janssen.com/johnson-johnson-announces-single-shot-janssen-covid-19-vaccine-candidate-met-primary-endpoints) (2021).
- 608 22 Edara, V. V. *et al.* Infection- and vaccine-induced antibody binding and neutralization of  
609 the B.1.351 SARS-CoV-2 variant. *Cell Host Microbe* **29**, 516-521.e513,  
610 doi:10.1016/j.chom.2021.03.009 (2021).
- 611 23 Wang, Z. *et al.* mRNA vaccine-elicited antibodies to SARS-CoV-2 and circulating  
612 variants. *Nature* **592**, 616-622, doi:10.1038/s41586-021-03324-6 (2021).
- 613 24 Wu, K. *et al.* Serum Neutralizing Activity Elicited by mRNA-1273 Vaccine. *N Engl J*  
614 *Med* **384**, 1468-1470, doi:10.1056/NEJMc2102179 (2021).
- 615 25 Wu, K. *et al.* mRNA-1273 vaccine induces neutralizing antibodies against spike mutants  
616 from global SARS-CoV-2 variants. *bioRxiv* **2021.01.25.427948**,  
617 doi:10.1101/2021.01.25.427948 (2021).
- 618 26 Azizi, A. *et al.* A combined nucleocapsid vaccine induces vigorous SARS-CD8+ T-cell  
619 immune responses. *Genet Vaccines Ther* **3**, 7, doi:10.1186/1479-0556-3-7 (2005).
- 620 27 Shang, B. *et al.* Characterization and application of monoclonal antibodies against N  
621 protein of SARS-coronavirus. *Biochemical and Biophysical Research Communications*  
622 **336**, 110-117, doi:<https://doi.org/10.1016/j.bbrc.2005.08.032> (2005).

- 623 28 Peng, H. *et al.* Long-lived memory T lymphocyte responses against SARS coronavirus  
624 nucleocapsid protein in SARS-recovered patients. *Virology* **351**, 466-475,  
625 doi:<https://doi.org/10.1016/j.virol.2006.03.036> (2006).
- 626 29 Narayanan, K., Chen, C.-J., Maeda, J. & Makino, S. Nucleocapsid-independent specific  
627 viral RNA packaging via viral envelope protein and viral RNA signal. *Journal of*  
628 *virology* **77**, 2922-2927, doi:10.1128/jvi.77.5.2922-2927.2003 (2003).
- 629 30 Zeng, W. *et al.* Biochemical characterization of SARS-CoV-2 nucleocapsid protein.  
630 *Biochemical and biophysical research communications*, S0006-0291X(0020)30876-  
631 30877, doi:10.1016/j.bbrc.2020.04.136 (2020).
- 632 31 Grifoni, A. *et al.* Targets of T Cell Responses to SARS-CoV-2 Coronavirus in Humans  
633 with COVID-19 Disease and Unexposed Individuals. *Cell* **181**, 1489,  
634 doi:10.1016/j.cell.2020.05.015 (2020).
- 635 32 Le Bert, N. *et al.* SARS-CoV-2-specific T cell immunity in cases of COVID-19 and  
636 SARS, and uninfected controls. *Nature* **584**, 457, doi:10.1038/s41586-020-2550-z (2020).
- 637 33 Sekine, T. *et al.* Robust T cell immunity in convalescent individuals with asymptomatic  
638 or mild COVID-19. *Cell* **183**, 158, doi:10.1101/2020.06.29.174888 (2020).
- 639 34 Altmann, D. M. & Boyton, R. J. SARS-CoV-2 T cell immunity: Specificity, function,  
640 durability, and role in protection. *Sci Immunol* **5**, eabd6160,  
641 doi:10.1126/sciimmunol.abd6160 (2020).
- 642 35 Chen, Z. & John Wherry, E. T cell responses in patients with COVID-19. *Nat Rev*  
643 *Immunol* **20**, 529-535, doi:10.1038/s41577-020-0402-6 (2020).
- 644 36 Matloubian, M., Concepcion, R. J. & Ahmed, R. CD4+ T cells are required to sustain  
645 CD8+ cytotoxic T-cell responses during chronic viral infection. *Journal of virology* **68**,  
646 8056-8063, doi:10.1128/jvi.68.12.8056-8063.1994 (1994).
- 647 37 Laidlaw, B. J., Craft, J. E. & Kaech, S. M. The multifaceted role of CD4(+) T cells in  
648 CD8(+) T cell memory. *Nat Rev Immunol* **16**, 102-111, doi:10.1038/nri.2015.10 (2016).
- 649 38 Elbe, S. & Buckland-Merrett, G. Data, disease and diplomacy: GISAID's innovative  
650 contribution to global health. *Glob Chall* **1**, 33-46, doi:10.1002/gch2.1018 (2017).
- 651 39 Vita, R. *et al.* The Immune Epitope Database (IEDB): 2018 update. *Nucleic Acids Res* **47**,  
652 D339-D343, doi:10.1093/nar/gky1006 (2019).
- 653 40 Amalfitano, A. *et al.* Production and Characterization of Improved Adenovirus Vectors  
654 with the E1, E2b, and E3 Genes Deleted. *Journal of virology* **72**, 926,  
655 doi:10.1128/JVI.72.2.926-933.1998 (1998).
- 656 41 Tan, C. W. *et al.* A SARS-CoV-2 surrogate virus neutralization test based on antibody-  
657 mediated blockage of ACE2-spike protein-protein interaction. *Nat Biotechnol* **38**, 1073-  
658 1078, doi:10.1038/s41587-020-0631-z (2020).
- 659 42 Kasinrerk, W., Baumruker, T., Majdic, O., Knapp, W. & Stockinger, H. CD1 molecule  
660 expression on human monocytes induced by granulocyte-macrophage colony-stimulating  
661 factor. *The Journal of Immunology* **150**, 579-584 (1993).
- 662 43 GISAID. SARS-CoV-2 Lineages. *GISAID.org* <https://www.gisaid.org> (2020-2021).
- 663 44 Nakamura, S. & Yoshimori, T. New insights into autophagosome-lysosome fusion. *J Cell*  
664 *Sci* **130**, 1209-1216, doi:10.1242/jcs.196352 (2017).
- 665 45 Lőrincz, P. & Juhász, G. Autophagosome-Lysosome Fusion. *J Mol Biol* **432**, 2462-2482,  
666 doi:10.1016/j.jmb.2019.10.028 (2020).
- 667 46 Kabeya, Y. *et al.* LC3, a mammalian homologue of yeast Apg8p, is localized in  
668 autophagosome membranes after processing. *Embo j* **19**, 5720-5728,  
669 doi:10.1093/emboj/19.21.5720 (2000).

- 670 47 Schmid, D., Pypaert, M. & Münz, C. Antigen-loading compartments for major  
671 histocompatibility complex class II molecules continuously receive input from  
672 autophagosomes. *Immunity* **26**, 79-92, doi:10.1016/j.immuni.2006.10.018 (2007).
- 673 48 Patterson, N. L. & Mintern, J. D. Intersection of autophagy with pathways of antigen  
674 presentation. *Protein & Cell* **3**, 911-920, doi:10.1007/s13238-012-2097-3 (2012).
- 675 49 Crotzer, V. L. & Blum, J. S. Autophagy and Its Role in MHC-Mediated Antigen  
676 Presentation. *The Journal of Immunology* **182**, 3335, doi:10.4049/jimmunol.0803458  
677 (2009).
- 678 50 You, L. *et al.* The crosstalk between autophagic and endo-/exosomal pathways in antigen  
679 processing for MHC presentation in anticancer T cell immune responses. *Journal of*  
680 *Hematology & Oncology* **10**, 165, doi:10.1186/s13045-017-0534-8 (2017).
- 681 51 Peng, Y. *et al.* Broad and strong memory CD4(+) and CD8(+) T cells induced by SARS-  
682 CoV-2 in UK convalescent individuals following COVID-19. *Nat Immunol* **21**, 1336-  
683 1345, doi:10.1038/s41590-020-0782-6 (2020).
- 684 52 Rice, A. *et al.* The Dual-Antigen Ad5 COVID-19 Vaccine Delivered as an Intranasal Plus  
685 Subcutaneous Prime Elicits Th1 Dominant T-Cell and Humoral Responses in CD-1 Mice.  
686 *bioRxiv* **2021.03.22.436476**, doi:10.1101/2021.03.22.436476 (2021).
- 687 53 Tilocca, B. *et al.* Comparative computational analysis of SARS-CoV-2 nucleocapsid  
688 protein epitopes in taxonomically related coronaviruses. *Microbes Infect*, S1286-  
689 4579(1220)30053-30058, doi:10.1016/j.micinf.2020.04.002 (2020).

691

692

693

694

695

696

697

698

699

700

701

702

703

704

705

706

## SUPPLEMENTARY MATERIALS for

707

708 **Prime hAd5 Spike + Nucleocapsid Vaccination Induces Ten-Fold Increases in Mean T-Cell**

709 **Responses in Phase 1 Subjects that are Comparable COVID-19 Convalescents and**

710 **Sustained Against Spike Variants**

711

### Supplementary Materials

713

#### Methods

715

##### *Quantification of anti-SARS-CoV-2 spike antibodies in plasma*

717

718 The presence of anti-SARS-CoV-2 spike antigen antibodies in previously infected patient  
719 plasma used in studies here was validated. IgG against SARS-CoV-2 spike was detected in plasma  
720 using ELISA. Briefly, EIA/RIA plates were coated with a solution of purified recombinant SARS-  
721 CoV-2-derived Spike protein (1µg/ml, S-Fusion. ImmunityBio, Inc.) suspended in coating buffer  
722 (0.05 M carbonate-bicarbonate, pH 9.6) and incubated overnight at 4°C. Plates were washed three  
723 times with TPBS solution (PBS + 0.05% Tween 20). Blocking solution (2% non-fat milk in TPBS)  
724 was added and incubated at room temperature (RT, 1h). Serial dilutions of plasma were prepared  
725 in 1% non-fat milk in TPBS. Plates were washed as described above and serial dilutions of plasma  
726 were added to the plate and incubated at RT (1h). Plates were washed three times. Goat anti-  
727 Human IgG (H+L) HRP-conjugated secondary antibody (1:6000 dilution) prepared in 1% non-fat  
728 milk/TPBS was added and incubated at RT (1h). Plates were washed three times. Substrate  
729 (3,3',5,5'-tetramethylbenzidine (TMB)) was added to each well and incubated at RT (10min). The  
730 reaction was stopped by addition of sulfuric acid (1N H<sub>2</sub>SO<sub>4</sub>). The optical density (450 nm) was  
731 measured by a Synergy 2 (BioTek Instruments, Inc.) plate reader. Data were analyzed using Prism  
732 8 (GraphPad Software, LLC).

733

##### *cPass<sup>TM</sup> neutralizing antibody detection*

735

736 The GenScript cPass<sup>TM</sup> (<https://www.genscript.com/cpass-sars-cov-2-neutralization-antibody-detection-Kit.html>) kit for detection of neutralizing antibodies was used according to the  
737 manufacturer's instructions.<sup>41</sup> The kit detects circulating neutralizing antibodies against SARS-  
738 CoV-2 that block the interaction between the S RBD with the ACE2 cell surface receptor. It is  
739 suitable for all antibody isotypes.

741

742 To evaluate the levels of anti-SARS-CoV-2 neutralizing antibodies in plasma, dilutions of  
743 plasma were incubated with horseradish peroxidase-conjugated spike RBD (37°C, 30min). The  
744 RBD-plasma mixture was added to a microtiter plate coated with ACE2 and incubated at 37°C (15  
745 min). Plates were washed and substrate (TMB) added at room temperature (15 min). The reaction  
746 was stopped and plates read on a plate reader at 450 nm.

747

##### *Live virus assay of plasma neutralization of infection*

749

750 The ability of previously SARS-CoV-2 infected patient plasma used in studies here to  
751 neutralize SARS-CoV-2 infection *in vitro* was also validated. All aspects of the assay utilizing  
752 virus were performed in a BSL3 containment facility according to the ISMMS Conventional

753 Biocontainment Facility SOPs for SARS-CoV-2 cell culture studies. Vero E6 kidney epithelial  
754 cells from *Cercopithecus aethiops* (ATCC CRL-1586) were plated (20,000 cells/well) in a 96-well  
755 format and 24 hours later, cells were incubated with antibodies or heat inactivated plasma  
756 previously serially diluted in 3-fold steps in DMEM containing 2% FBS, 1% NEAAs, and 1%  
757 Pen-Strep; the diluted samples were mixed 1:1 with SARS-CoV-2 in DMEM containing 2% FBS,  
758 1% NEAAs, and 1% Pen-Strep at 10,000 TCID<sub>50</sub>/mL for 1 hr at 37°C, 5% CO<sub>2</sub>. This incubation  
759 did not include cells to allow for neutralizing activity to occur prior to infection. For detection of  
760 neutralization, the virus/sample mixture (120 µL) was transferred to the Vero E6 cells and  
761 incubated (48 hours) before fixation with 4% PFA. Each well received virus (60 µl) or an infectious  
762 dose of 600 TCID<sub>50</sub>. Control wells, including six wells on each plate for no virus and virus-only  
763 controls, were used. The percent neutralization was calculated as 100-((sample of interest-[average  
764 of “no virus”])/[average of “virus only”])\*100) with a stain for CoV-2 Np imaged on a Celigo  
765 Imaging Cytometer (Nexcelom Bioscience).

766

#### 767 *Transfection of HEK 293T cells and detection of plasma antibody binding*

768

769 To assess binding of plasma from a previously infected patient to antigens expressed by hAd5  
770 S-Fusion and hAd5 S-Fusion + N-ETSD vaccines, plasma was incubated with construct-  
771 transfected HEK 293T cells and binding determined by flow cytometry. HEK 293T cells (2.5 x  
772 10<sup>5</sup> cells/well in 24 well plates) were grown in DMEM (Gibco) with 10% FBS and 1X PSA (100  
773 units/mL penicillin, 100 µg/mL streptomycin, 0.25 µg/mL Amphotericin B) at 37°C. Cells were  
774 either left untransfected or were transfected with 0.5 µg of S-Fusion or S-Fusion + N-ETSD hAd5  
775 plasmid DNA using a JetPrime transfection reagent (Polyplus) according to the manufacturer’s  
776 instructions. Twenty-four hours later, cells were incubated for 30 min. with previously infected  
777 patient or healthy (unexposed, UnEx) plasma that had been serially diluted 10-fold for 30 min.  
778 Plasma IgG was labeled using a goat anti-human IgG-phycoerythrin conjugated and labeled cells  
779 were acquired using the Thermo-Fisher Attune NxT flow cytometer and analyzed using FlowJo  
780 Software to determine Mean Fluorescence Intensity (MFI) values of both the untransfected and  
781 transfected cells. Results were graphed as the difference in MFI between untransfected and  
782 transfected cells for the S-Fusion and S-Fusion + N-ETSD constructs over the plasma dilutions.

783

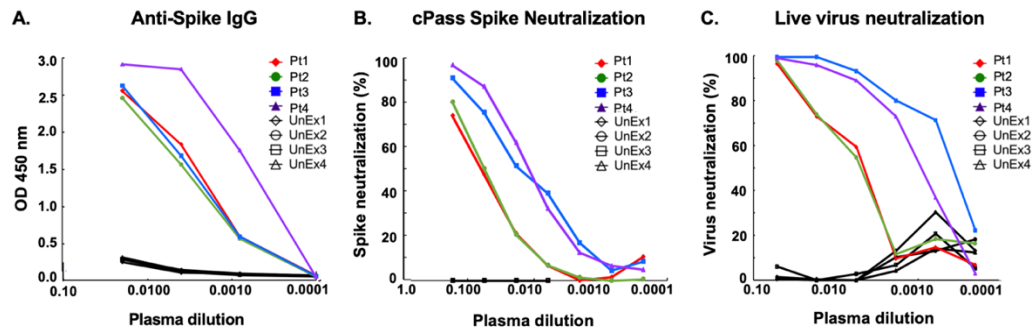
## 784 **Results**

785

### 786 *Previously SARS-CoV-2-infected patient plasma confirmed to have neutralizing anti-S antibodies*

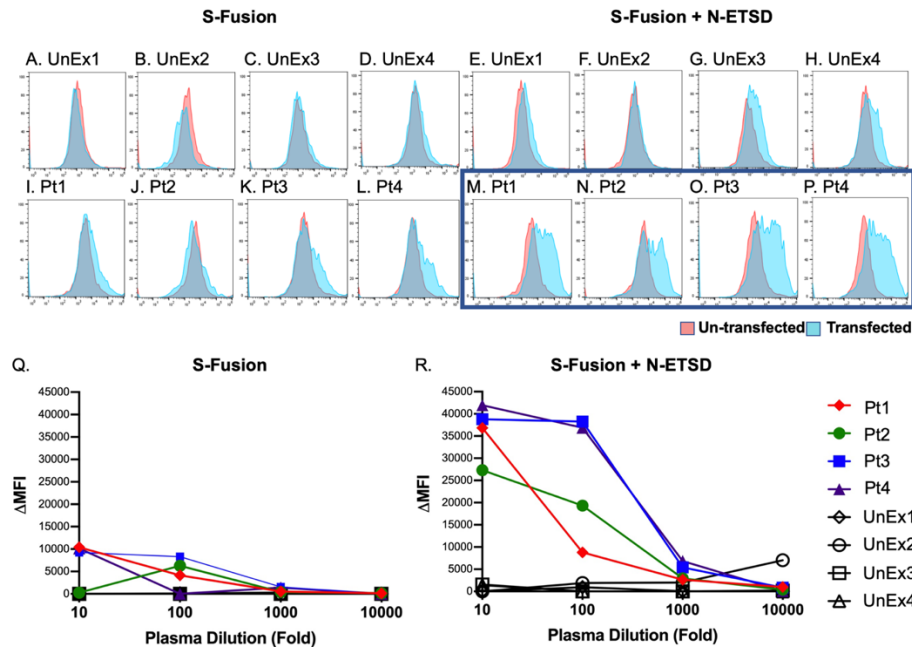
787

788 For the studies described below, plasma samples were collected from four individuals  
789 convalescing from SARS-CoV-2 infection as confirmed by antibody assays and patient history as  
790 described Methods. The presence of anti-Spike IgG, and of neutralizing antibodies by both a  
791 surrogate SARS-CoV-1 neutralization assay<sup>41</sup> and live virus assays, were confirmed in all patient  
792 samples (Suppl. Fig. S1). Samples were also collected from four virus-naïve individuals and were  
793 used as controls.



794  
 795 **Fig. S1** Plasma samples from patients (Pt) previously infected with SARS-CoV-2 contain  
 796 neutralizing antibodies. (A) The levels of anti-spike IgG as determined by OD at 450 nm are  
 797 shown. (B) All four Pt plasma samples contained antibodies that blocked RBD-ACE2 binding and  
 798 (C) contained SARS-CoV-2 neutralizing antibodies.  
 799 *Previously SARS-CoV-2-infected patient plasma binds to vaccine-transfected HEK-293T cells*  
 800

801 In additional studies to validate immune responses to SARS-CoV-2 antigens, the binding of  
 802 previously SARS-CoV-2 infected patient and virus-naïve control individual plasma to human  
 803 embryonic kidney (HEK) 293T cells transfected with either hAd5 S-Fusion alone or hAd5 S-  
 804 Fusion + N-ETSD was assessed (Suppl. Fig. S2). This binding reflects the presence of antibodies  
 805 in plasma that recognize antigens expressed by the hAd5 vectored vaccines. Quantification of  
 806 histograms showed little or no binding of virus-naïve plasma antibodies to cells expressing either  
 807 construct, and the highest binding of plasma antibodies from a previously SARS-CoV-2 infected  
 808 patient to cells expressing the dual antigen S-Fusion + N-ETSD construct (Suppl. Fig. S2R).



809  
 810 **Fig. S2** Plasma from previously SARS-CoV-2 infected patients shows greater binding to S-Fusion  
 811 + N-ETSD surface antigens compared to S-Fusion alone after transfection of HEK 293T cells.  
 812 HEK 293T cells that were either uninfected (pink) or infected (blue) with S-Fusion alone or  
 813 bivalent S-Fusion + N-ETSD were exposed to plasma from either unexposed (UnEx) controls or  
 814 previously infected SARS-CoV-2 patients (Pt). Flow histograms for (A-D) UnEx with S-Fusion;  
 815 (E-H) UnEx with S-Fusion + N-ETSD; (I-L) Pt with S-Fusion; and (M-P) Pt with S-Fusion + N-  
 816 ETSD, all n = 4, are shown. When the  $\Delta$ MFI (difference in binding to transfected versus



817 untransfected cells) is graphed, it is apparent that compared to (Q) S-Fusion, (R) binding of Pt  
 818 plasma to S-Fusion + N-ETSD transfected cells is much higher and that plasma from UnEx  
 819 individuals shows little binding.

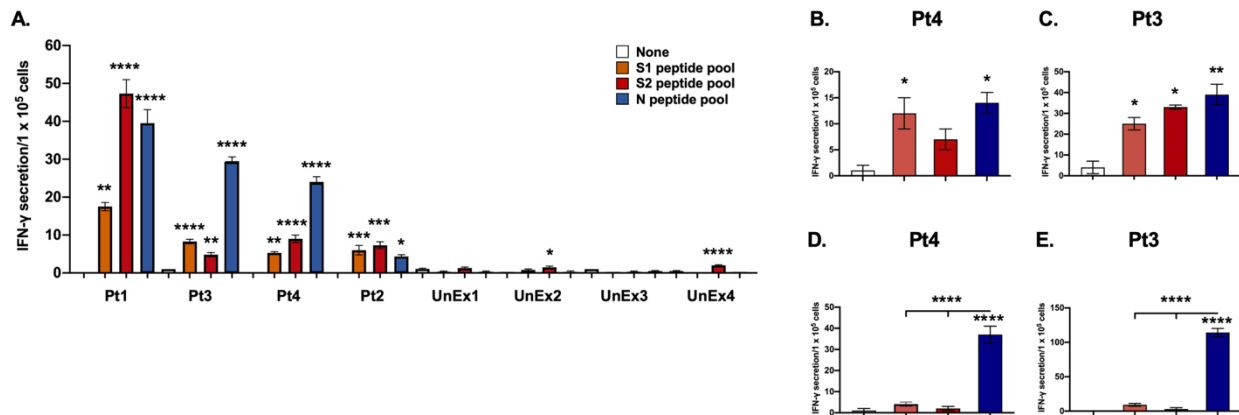
820

821 *Previously SARS-CoV-2-infected patient T cells are activated by S and N peptide pools*

822

823 The reactivities of T cells from the previously SARS-CoV-2-infected patients was confirmed  
 824 by incubation with S1 (containing the spike receptor binding domain), S2 and N peptides pools  
 825 (Fig. S3A). The specific reactivities of CD4+ (Fig. S3B and C) and CD8+ T cells was then  
 826 determined, showing CD8+ T cells were more selectively activated by the N peptide pool.

827



828

829 **Fig. S3.** *T-cell responses to MoDCs pulsed with SARS-CoV-2 peptides.* Unselected T cells from  
 830 all four previously SARS-CoV-2 infected patients (Pt) show significant IFN- $\gamma$  responses to S1, S2,  
 831 and N peptide pool-pulsed MoDCs as compared to 'none'. T cells from virus-naïve (unexposed,  
 832 UnEx) control individuals showed far lower responses. Statistical analysis performed using One-  
 833 way ANOVA and Tukey's post-hoc analysis for samples from each patient compared only to  
 834 'none' where \*  $p < 0.05$ , \*\*  $p < 0.01$ , \*\*\*  $p < 0.001$ , and \*\*\*\*  $p < 0.0001$ . Data graphed as the mean  
 835 and SEM;  $n = 3-4$ . Patient MoDCs pulsed with SARS-CoV-2 peptide mixes overnight were  
 836 incubated with autologous CD4+ (B, Pt 4; C, Pt 3) or CD8+ (D, Pt 4; E, Pt 3) T cells. IFN- $\gamma$  levels  
 837 were determined by ELISpot. Statistical analysis performed using One-way ANOVA and  
 838 Dunnett's post-hoc multiple comparison analysis to compare each peptide pool to Veh (shown  
 839 above the bar) or between peptide pools (above line) where \*  $p < 0.05$ , \*\*  $p < 0.01$  and  
 840 \*\*\*\*  $p < 0.00001$ . Data graphed as mean and SEM;  $n = 3$ .